Spatial and temporal correlations of spike trains in frog retinal ganglion cells

Wen-Zhong Liu · Wei Jing · Hao Li · Hai-Qing Gong · Pei-Ji Liang

Abstract For a neuron, firing activity can be in synchrony with that of others, which results in spatial correlation; on the other hand, spike events within each individual spike train may also correlate with each other, which results in temporal correlation. In order to investigate the relationship between these two phenomena, population neurons' activities of frog retinal ganglion cells in response to binary pseudo-random checker-board flickering were recorded via a multi-electrode recording system. The spatial correlation index (*SCI*) and temporal correlation index (*TCI*) were calculated for the investigated neurons. Statistical results showed that, for a single neuron, the *SCI* and *TCI* values were highly related—a neuron with a high *SCI* value generally had a high *TCI* value, and these two indices were both associated with burst activities in spike train of the investigated neuron. These results may suggest that spatial and temporal correlations of single neuron's spiking activities could be mutually modulated; and that burst activities could play a role in the modulation. We also applied models to test the contribution of spatial and temporal correlations for visual information processing. We show that a model considering spatial and temporal correlations could predict spikes more accurately than a model does not include any correlation.

Keywords Ganglion cell · Spatial correlation · Temporal correlation · Multi-electrode recording · Burst activities

Action Editor: Simon R Schultz

W.-Z. Liu · W. Jing · H. Li · H.-Q. Gong · P.-J. Liang (✉)
Department of Biomedical Engineering,
Shanghai Jiao Tong University,
800 Dong-Chuan Road,
Shanghai 200240, China
e-mail: pjliang@sjtu.edu.cn

Abbreviations

ISI	inter-spike-intervals
RGC	retinal ganglion cell
MEA	multi-electrode array
SCI	spatial correlation index
STA	Spike-triggered averaged
TCI	temporal correlation index
LGN	lateral geniculate nucleus

1 Introduction

Retinal ganglion cells (RGCs) encode visual information via their population activities (Brivanlou et al. 1998; Meister et al. 1995; Schnitzer and Meister 2003); in other words, ganglion cells' activities are spatially correlated. It was noted that different neurons in a retina may correlate with different numbers of other neurons and with different strengths (Schnitzer and Meister 2003), indicating that neurons may differ in their spatial correlation. In addition to spatial patterns, temporal patterns of single neuron's spike activities were also extensively studied. It was reported that temporal correlation patterns exist within single spike trains in various parts of the nervous system, such as visual system (Teich et al. 1996), auditory system (Lowen and Teich 1992) and hippocampus (Bhattacharya et al. 2005). The existence of temporal correlation in a spike sequence indicates that spike events should not be totally independent of each other.

While spatial correlation among spike trains reflects connected network state (Meister et al. 1995; Schneidman et al. 2006; Schnitzer and Meister 2003), temporal correlation within a single spike train might be related to activity modulation and information storage. In macaque

monkey, it was reported that the spatial and temporal correlations contributed to information coding and transmission from retina to central visual systems (Pillow et al. 2008). It was also found that in hippocampus, spatial correlations among neurons were often accompanied by long-range temporal correlation within the single spike trains (Bhattacharya et al. 2005).

In the present study, we recorded activities from populations of RGCs in response to pseudo-random checker-board flickering by using a multi-electrode array (MEA). In order to investigate the relationship between spatial and temporal correlations in RGCs, spatial correlation index (SCI) and temporal correlation index (TCI) were calculated. It was found that for a single neuron, these two indices were highly correlated, with both being associated with burst activities in spike trains: a spike sequence with higher burst fraction (percentage of burst activities in a spike train) normally had larger spatial and temporal correlation indices. Our findings of highly correlated SCI and TCI in single neuron's activity may suggest the existence of mutual modulation of spatial and temporal correlations in retina, and this modulation may contribute to retinal information processing.

To investigate the contribution of spatial and temporal correlations in the retinal information processing, we further adopted two models proposed by Pillow et al. (Pillow et al. 2008), and tested the model prediction performance. It turned out that the Coupled Model considering spatial and temporal correlations could predict spikes with higher accuracy than the Linear-Nonlinear Model which does not include any spatial or temporal correlation.

2 Methods and materials

2.1 Experiment

2.1.1 Surgery

Before experiment, bullfrog was dark adapted for at least 30 min. The bullfrog was then double pithed and its eyes were enucleated under dim red light. Separated eyeball was hemisected, the eyecup was cut into small pieces, and then the retina was isolated carefully. All procedures strictly conformed to the humane treatment and use of animals prescribed by the Association for Research in Vision and Ophthalmology.

2.1.2 Electrode recording

Neuronal activities were recoded extracellularly by multi-electrode arrays (MEA, MMEP-4, CNNS UNT, USA),

which consisted of 64 electrode (8 μm in diameter) arranged in an 8×8 matrix with 150 μm tip-to-tip distances between adjacent electrodes horizontally and vertically. After surgery, a small patch (4×4 mm^2) of isolated retina was placed on MEA with the ganglion cell side contacting the electrodes. The oxygenated (95% O_2 and 5% CO_2) standard perfusate contained (in mM): NaCl 100.0, KCl 2.5, MgCl$_2$ 1.6, CaCl$_2$ 2.0, NaHCO$_3$ 25.0, glucose 10.0.

Recorded signals were firstly amplified through a 64-channel amplifier (MEA workstation, Plexon Inc. Texas, USA) and were sampled at a rate of 40 kHz for each individual channel and then stored in a Pentium-IV-based computer (Jing et al. 2010a). Timing signals of visual stimulus were also recorded and stored in the computer. Spike sorting was performed by using method proposed by Zhang et al. (Zhang et al. 2004), as well as the spike-sorting unit in the commercial software OfflineSorter (Plexon Inc. Texas, USA). Only single-neuronal events clarified by both spike-sorting methods mentioned above were used for further analyses. In our experiments using MEA with 150 μm spacing, although there was little chance for spikes from one neuron to be recorded by two electrodes, the method proposed by Segev et al. (Segev et al. 2004) was also applied to make sure that any two sequences under investigation were not from the same neuron.

2.1.3 Visual stimulation

In the frog retina, RGCs can be classified into four subtypes based on their response properties: dimming detectors, sustained contrast detectors, net convexity detectors and moving-edge detectors (Lettvin et al. 1959). Light-Off stimulus evokes Off-sustained spike discharges in the dimming detectors but elicits only a few spike discharges transiently in other cell subtypes (Ishikane et al. 2005). In our experiments, we applied 1-s On / 9-s Off (repeated 30 times) full field white-light to evoke response of RGCs. Light stimulus was applied via a computer monitor (Iiyama, Vision Master Pro 456, Japan) and was focused to form a 1.1×1.1 mm^2 image on the isolated retina through a lens system. Dimming detectors could be identified according to their response. In this study, only dimming detectors were selected for further analyses.

In order to study the intrinsic correlation characteristics of neuronal activities, we applied pseudo-random checker-board flickering sequence as visual stimulus (Reid et al. 1997). Pseudo-random checker-board which consisted of 16×16 sub-squares was displayed on the computer monitor and refreshed at a frame rate of 20 Hz. Each sub-square covered an area of 66×66 μm^2 on the retinal piece and was assigned a value either "+1" (white light,

77.7 nW/cm^2) or "−1" (dark) following a pseudo-random binary sequence (Jing et al. 2010b). The flickering stimulation was lasted for 300 s. During such a period, the spikes elicited from a single neuron could be up to around 1000, which was adequate for mapping the RGC's receptive field. The power spectra of the stimulus applied in our experiment were also calculated, the results of which revealed that the stimulus is overall random, both temporally and spatially (Cai et al. 2008). Experiments were performed on 4 retinas.

$$f(x,y) = A\exp\left(-0.5\left\{\left[\frac{(x-x_c)\cos\theta - (y-y_c)\sin\theta}{\sigma_x}\right]^2 + \left[\frac{(x-x_c)\sin\theta + (y-y_c)\cos\theta}{\sigma_y}\right]^2\right\}\right) \qquad (1)$$

where (x_c, y_c) is the position of the estimated mass center of the receptive field, (x, y) is the position of the stimulus, A is the estimated maximum amplitude of the two-dimensional Gaussian distribution, θ is the angle between the major axis (long axis) of the receptive field and the x axis. σ_x and σ_y are the standard deviation of the major and minor axes of the two-dimensional Gaussian distribution respectively. The profile of an example neuron's receptive field is plotted in Fig. 1. Neuron subtype can be confirmed by analyzing the cell's receptive field properties.

2.2.2 Spatial correlation strength

Spatial correlation strength (Meister et al. 1995; Schnitzer and Meister 2003) was calculated as the ratio between the probability of observed correlated spikes and that expected by chance. Briefly speaking, spike trains were binned to "0–1" sequence with resolution of 20 ms, with "1" being a bin with spike(s), and "0" for none; then in the i-th spike train, the probability for a bin with spike(s) is P_i. For two
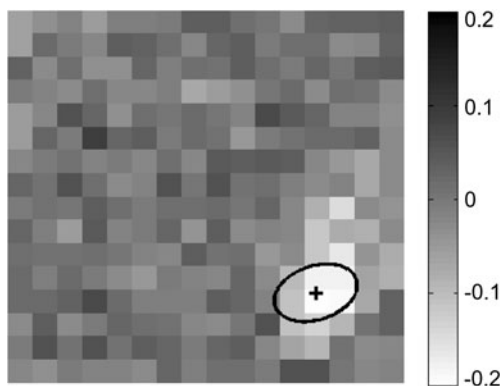

Fig. 1 Receptive field profile of an example neuron. The black cross indicates the estimated mass center of its receptive field; the border is 1-s.d. ellipse

2.2 Data analysis

2.2.1 Receptive field properties

The ganglion cells' receptive field properties were estimated using spike-triggered average (STA) method proposed by Meister et al (Meister et al. 1994), a two dimensional Gaussian distribution was fitted to the original estimation (Devries and Baylor 1997; Meister et al. 1995; Schnitzer and Meister 2003):

binned spike trains A and B, the probability of observed correlated spikes P_{AB} could be obtained by multiplying A and B to obtain a new sequence AB and calculating the percentage of bins with "1" in sequence AB, while the probability that expected by chance was $P_A P_B$. Correlation strength is defined as:

$$C_s = \frac{P_{AB}}{P_A P_B} \qquad (2)$$

2.2.3 Spatial correlation index

To estimate the strength of spatial correlation between a particular neuron and its neighboring ones, we first calculated the correlation coefficient between pair-wise neurons following the way proposed by Schnitzer et al. (Schnitzer and Meister 2003):

$$S_{AB} = P_{AB}\log_2(P_{AB}/P_A P_B) \qquad (3)$$

Generally speaking, strongly concerted pair has large S_{AB} value.

During our analysis, a neuron was selected for spatial correlation index analysis if, in its neighboring area with a radius of 400 μm, there were more than 8 neurons' activities being successfully recorded during the experiment. Spatial correlation index of neuron A (SCI_A) can be estimated as the average correlation coefficient over all neuron pairs that neuron A takes part in:

$$SCI_A = \frac{1}{N}\sum_{k=1}^{N} S_{Ak} \qquad (4)$$

Where N is the number of recorded cells in neuron A's neighboring area with a radius of 400 μm.

To test the significance of the SCI values, we generated "shuffled" data by shuffling each spike train in the group

(for both the neuron under investigation and its neighbors) by a different random length of time delay ($0 < \Delta t < 1$ s). This shuffling procedure maintains the temporal structure of the spike sequences, yet disturbs the original correlated firings among neurons (Oram et al. 1999). Then we calculated the *SCI* index for the "shuffled" data $SCI_{shuffle}$. We repeated the shuffling procedure for 100 times for each data set, and obtained 100 distributed SCI_{shuff} values. The difference between the *SCI* values calculated for the original spike sequences and the "shuffled" data is defined as: $Z = (SCI- <\{SCI_{shuff}\}>)/std(\{SCI_{shuff}\})$; where *SCI* is the value of original sequence, $\{SCI_{shuff}\}$ are the values calculated using the 100 sets of "shuffled" sequences, $<\bullet>$ is the mean value, and $std(\bullet)$ represents the standard deviation. When $\{SCI_{shuff}\}$ follows a Gaussian distribution (It was confirmed that the hypothesis that $\{SCI_{shuff}\}$ of our "shuffled" data follows a Gaussian can not be rejected at the 5% significance level by Jarque-Bera test), $Z>1.96$ signifies the rejection of null hypothesis that the original spike sequence is independent of its adjacent neurons' activities (no spatial correlation) at 5% significance level (Bhattacharya et al. 2005).

2.2.4 Temporal correlation index

Temporal correlation index was estimated based on entropy method (Reinagel and Reid 2000; Strong et al. 1998). A spike train was binned to "0-1" sequence with resolution of 2 ms (to ensure that each bin has no more than 1 spike), with "1" implying spike and "0" for none. Initially, we made an assumption that the firing activities were temporally uncorrelated, and used 1-bin length "word" to calculate the entropy of the spike train H_M:

$$H_M = -P_1 \log_2 P_1 - P_0 \log_2 P_0 \qquad (5)$$

However, the real entropy of the spike train H_r is different from H_M when the spike train is temporally correlated (Reinagel and Reid 2000). The temporal correlation index TCI can thus be calculated as:

$$TCI = H_M - H_r \qquad (6)$$

where the real entropy H_r can be estimated following the method introduced by Strong et al (Strong et al. 1998). Briefly, we calculated entropy with word length ≥2 bins and plotted the entropy values against the reciprocals of word length, the linear part of which can be fitted as:

$$H(n) = H_r + \frac{H_1}{n} + \frac{H_2}{n^2} \qquad (7)$$

where n is the word length, $H(n)$ is the calculated entropy, and H_r is the estimated real entropy (see Fig. 2); $\frac{H_1}{n}$ and $\frac{H_2}{n^2}$
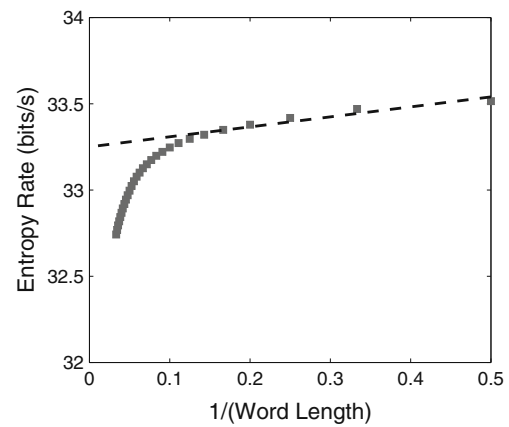

Fig. 2 Estimate of real entropy of a spike train. Entropy values estimated using different word-lengths are plotted against the reciprocals of word-length. Dash line indicates extrapolation to infinite word-length. Intersect of the dash line on Y-axis is considered as real entropy of the spike train

are corrections for the bias of estimated entropy owing to finite data set (Strong et al. 1998).

Insufficient data may lead to biased results for entropy estimation, thus we followed the way proposed by Strong et al (Strong et al. 1998) to ascertain data adequacy. Briefly, we used different fraction of data for entropy estimation, and then extrapolated the result for infinite data size. The data were accepted as adequate if the difference between extrapolated infinite-data size entropy and the calculated whole-sequence size entropy was less then 20% of the infinite-data size entropy (Strong et al. 1998). All data presented in this paper are adequate according to this criterion.

To test the significance of the *TCI* values, we compared the *TCI* values of the original spike trains with those of Poisson sequences with the same firing rates. Briefly, for each individual neuron, we generated 100 Poisson sequences with the same firing rate, and calculated the *TCI* value for each set of these generated sequences. Then, we calculated the difference between the *TCI* values of the original sequence and the surrogate data: $Z_T = (TCI- <\{TCI_{generate}\}>)/std(\{TCI_{generate}\})$; where *TCI* is the value calculated for the original spike sequence, $\{TCI_{generate}\}$ are the values calculated for 100 sets of the generated Poisson sequence with the same firing rate as the neuron to be examined, $<\bullet>$ denotes the mean value, and $std(\bullet)$ represents the standard deviation. If $\{TCI_{generate}\}$ follows a Gaussian distribution (it was confirmed that the hypothesis that $\{TCI_{generate}\}$ of our surrogate data follows a Gaussian distribution can not be rejected at 5% significance level by Jarque-Bera test), $Z_T>1.96$ signifies the rejection of null hypothesis that the original spike sequence follows a Poisson process at 5% significance level (Bhattacharya et al. 2005).

2.2.5 Fano factor

Within a spike train, temporal correlation may occur with different time scales, some temporal correlation appears in a range up to tens of seconds (Teich et al. 1997), whilst spikes within a burst are correlated with a range only up to tens of milliseconds (Lisman 1997). To investigate correlation with what time scale accounts for the *TCI* value of the spiking sequence, we calculated Fano factor values of a spike train with different counting time windows, from 10 ms to 25 s.

The Fano factor $F(T)$ is defined as:

$$F(T) = \frac{\text{var}(N_i(T))}{\langle N_i(T) \rangle} \qquad (8)$$

where $N_i(T)$ is the number of events in the i-th counting window at time T, var(•) denotes the variance, and <•> represents the mean value. If a time series follows a Poisson process, which means that there is no temporal correlation within the process, the relevant $F(T)$ value should be equal to "1". An $F(T)$ value bigger than "1" indicates increased clustering of spikes than that expected for a Poisson process, and this is noted as positive correlation; while an $F(T)$ value smaller than "1" indicates negative correlation (Lowen and Teich 1992).

2.2.6 Correlation and model prediction

To test whether spatial and temporal correlations play any role in retinal information processing, we applied two models described by Pillow et al. (Pillow et al. 2008)—the Coupled Model, and the Linear-Nonlinear Model—to predict the occurrence of spikes and compared their prediction performance. While the Linear-Nonlinear Model captures merely single neuron's receptive field characteristics, the Coupled Model, which also contains a post-spike filter and a set of coupling filters, captures the spatial and temporal correlations among neurons' activities in addition to the single neuronal receptive field properties (all source codes were provided by Pillow; see http://pillowlab.cps. utexas.edu/code.html).

For testing spike prediction performance, we adopted 200 s experimental data to train the models, and the following 70 s data for testing the model prediction. We followed Pillow's method (Pillow et al. 2008) to calculate the model predictability of a spike train. Briefly, we initially estimated the log-likelihood of the Coupled model to generate spikes when a neuron really fired, which is denoted as P_c. We then calculated the log-likelihood P_n of a "null" model, which generates the spike in a sequence following a Poisson process with the same firing rate of the spike train, to generate spikes when the neuron fired. We

quantified the goodness of prediction as: $G = (P_n - P_c)/$ (number of real spikes).

3 Results

3.1 Spatial correlation

We first calculated the spatial correlation strength between any pairs of recorded ganglion cells, and plotted the spatial correlation strength values against the distance between the two cells' receptive field mass centers. Correlation strengths between neuron pairs of one example retina are shown in Fig. 3, which is evident that the correlation strength decreases as the distance increases, and correlation strength is very small when the distance is bigger than 400 μm (similar results were also obtained from the other 3 retinas, data not shown). Therefore, to better evaluate the strength of spatial correlation between a certain neuron and its neighboring ones, we selected a neuron ("selected" neuron) if, in its neighboring area with a radius of 400 μm, there were more than 8 neurons' ("adjacent" neurons) activities being successfully recorded during the experiment. *SCI* values were calculated for these selected neurons, as listed in Table 1. The numbers of the "adjacent" neurons related to each "selected" neuron are also listed.

The results listed in Table 1 show that the *SCI* values are spread in a wide range, the difference could be~10 fold. To test how significant the *SCI* values are, we generated the "shuffled" data and compared the difference between the *SCI* values calculated for the real experimental data set and the "shuffled" data set. In all the 55 neurons selected from 4 retinas, the Z values, which indicate the significance of
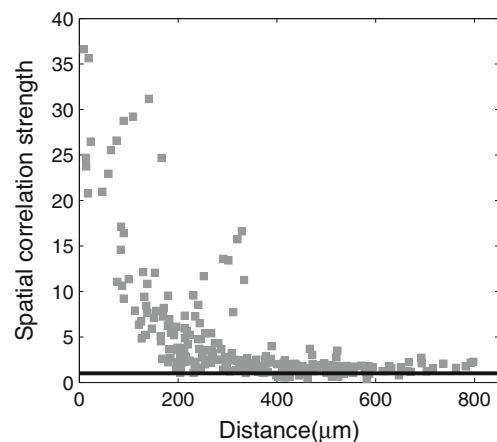

Fig. 3 Relationship between spatial correlation strength and inter-neuronal distance between pair-wise cells. Correlation strength is plotted against distance between receptive field mass centers of the neuron pairs. Black solid line: spatial correlation strength=1

Table 1 Summation of indices for all neurons under investigation

Retina	Neuron	SCI	(Z)	TCI	(Z_T)	Burst fraction fracfraction	N
#1	#11	0.018	(32.7)	2.077	(120)	0.228	20
	#12	0.016	(28.9)	1.823	(143)	0.222	20
	#13	0.011	(27.3)	1.359	(122)	0.166	21
	#14	0.011	(27.0)	1.027	(124)	0.177	19
	#15	0.009	(25.1)	0.994	(170)	0.175	20
	#16	0.010	(23.1)	0.719	(125)	0.134	20
	#17	0.003	(17.1)	0.638	(125)	0.131	22
	#18	0.005	(18.1)	0.517	(119)	0.139	15
	#19	0.004	(11.1)	0.376	(144)	0.099	15
	#110	0.004	(7.9)	0.343	(144)	0.091	14
	#111	0.001	(3.6)	0.232	(126)	0.056	8
#2	#21	0.009	(14.5)	1.785	(181)	0.146	20
	#22	0.007	(13.3)	1.733	(188)	0.145	22
	#23	0.004	(15.4)	0.868	(143)	0.097	23
	#24	0.004	(7.9)	0.645	(123)	0.074	22
	#25	0.002	(8.8)	0.506	(122)	0.106	14
	#26	0.002	(5.7)	0.500	(146)	0.062	14
	#27	0.001	(3.5)	0.482	(132)	0.073	21
	#28	0.001	(3.0)	0.390	(156)	0.063	21
#3	#31	0.007	(14.1)	0.398	(145)	0.079	17
	#32	0.006	(13.6)	0.333	(179)	0.065	11
	#33	0.002	(8.3)	0.217	(170)	0.060	14
	#34	0.002	(7.8)	0.194	(120)	0.039	12
	#35	0.005	(13.2)	0.197	(201)	0.053	13
	#36	0.003	(10.1)	0.186	(154)	0.046	8
	#37	0.003	(11.4)	0.184	(168)	0.031	9
	#38	0.006	(14.8)	0.169	(160)	0.025	10
	#39	0.001	(4.3)	0.108	(134)	0.040	22
	#310	0.003	(6.0)	0.087	(145)	0.039	12
	#311	0.002	(4.3)	0.082	(146)	0.026	20
	#312	0.003	(6.0)	0.079	(143)	0.020	9
	#313	0.001	(7.4)	0.071	(133)	0.011	11
#4	#41	0.011	(20.7)	1.578	(178)	0.146	28
	#42	0.007	(13.3)	1.081	(177)	0.165	25
	#43	0.006	(11.1)	1.059	(167)	0.128	23
	#44	0.006	(8.4)	1.021	(167)	0.164	17
	#45	0.007	(9.3)	0.941	(180)	0.139	18
	#46	0.008	(10.3)	0.940	(158)	0.099	24
	#47	0.007	(8.9)	0.671	(166)	0.123	10
	#48	0.008	(14.5)	0.665	(169)	0.077	22
	#49	0.006	(12.2)	0.663	(120)	0.112	25
	#410	0.006	(13.7)	0.463	(141)	0.051	21
	#411	0.004	(7.6)	0.419	(135)	0.077	8
	#412	0.004	(6.4)	0.391	(125)	0.048	24
	#413	0.007	(9.0)	0.381	(130)	0.060	14
	#414	0.006	(6.5)	0.336	(128)	0.061	19
	#415	0.006	(7.1)	0.328	(140)	0.051	25
	#416	0.002	(4.5)	0.170	(145)	0.051	12
	#417	0.004	(5.7)	0.166	(147)	0.047	23
	#418	0.003	(4.3)	0.131	(120)	0.033	25
	#419	0.003	(3.8)	0.124	(134)	0.055	17
	#420	0.003	(4.9)	0.114	(140)	0.038	25
	#421	0.002	(3.9)	0.082	(134)	0.010	10
	#422	0.002	(6.5)	0.054	(131)	0.006	23
	#423	0.005	(5.4)	0.052	(127)	0.027	8

N number of "adjacent" neurons

spatial correlation, are all over 1.96 as listed in Table 1. These results support the notion that these positive *SCI* values reflect the spatial correlation between the "selected" neurons and their neighbors, although the *SCI* values are quite small for some neurons (Bhattacharya et al. 2005).

3.2 Temporal correlation

TCI was calculated to estimate the temporal correlation within a spike train. It is calculated as the difference between the "maximum" entropy (obtained by assuming each spike is independent) and the real entropy (estimated as illustrated in Fig. 2) of a spike train. Similar to *SCI*, *TCI* values also vary among different neurons (see Table 1), with large value reflecting strong temporal correlation within a spike train, and vice versa.

TCI value should be equal to zero if there is no temporal correlation in a sequence, such as Poisson process; and for some neurons listed in Table 1, the *TCI* value were relatively small, at ~10^{-2}. So we tested whether the original spike trains were significantly different from Poison sequence as explained in the Methods and Materials parts. For all the 55 neurons recorded from 4 retinas in our experiments, the value of $Z_T \gg 1.96$, see Table 1, which is evidence for the existence of the temporal correlation.

Temporal correlation within a spike train may occur with different time scales. To test correlation in what time scale contributes more to the *TCI* value, we calculated the Fano factor values of single spike train with different counting time *T*. In order to identify whether the inter-spike-intervals (ISI) distribution or the ISI ordering is more important to the Fano factor value (Teich et al. 1996), we also randomly rearranged the ISI sequence of a single spike train, and then calculated the Fano factor values for the "shuffled" data sequence. For each spiking sequence, 100 "shuffled" data were produced, based on which the averaged Fano factor values were calculated.

Fano factor values of neurons' activities calculated for the example retina (#1) are plotted in Fig. 4(a). It is clear that neurons' *TCI* indices are more correlated with their Fano factor values when counting time is short (when time window is shorter than 600 ms, large *TCI* value is normally accompanied by big Fano factor values). The averaged Fano factor values calculated for the "shuffled" data are displayed in Fig. 4(b). It is clearly shown that the shuffling brings little change to Fano factor values for counting window shorter than 600 ms; but when counting window is longer than 600 ms, the shuffling procedure brings remarkable change to Fano factor values, as illustrated in Fig. 4(c). Similar results were also obtained from other 3 retinas (data not shown). This may suggest that temporal correlation in short time scales (≤ 600 ms)
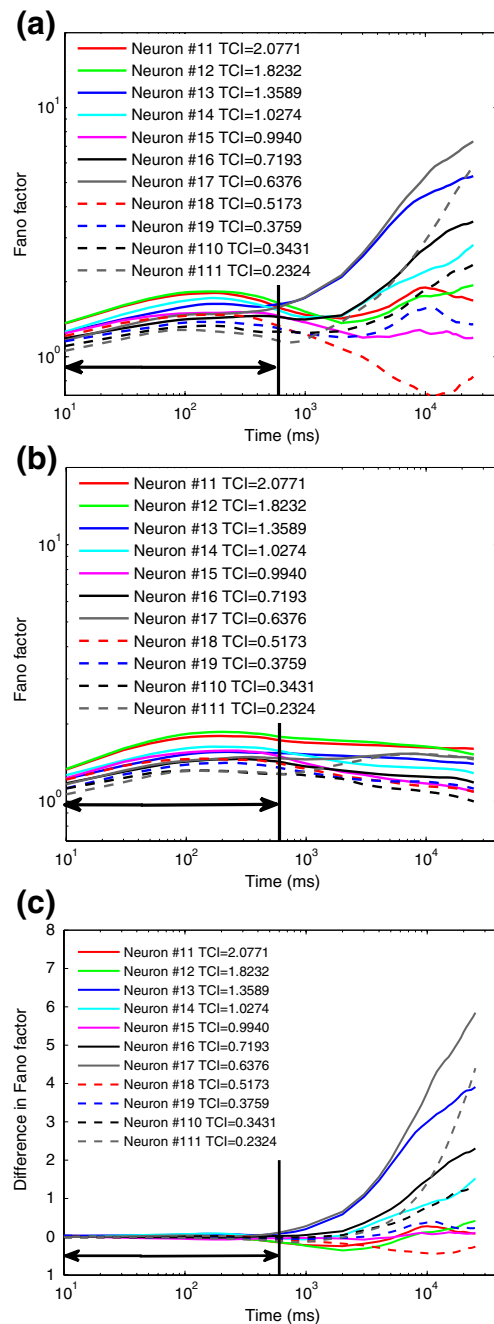

Fig. 4 Fano factor values calculated with time scales ranging from 10 ms to 25 s. (**a**) Fano factor values calculated for the original spike sequences. (**b**) Fano factor values calculated for the randomly shuffled data. (**c**) Difference between Fano factor values plotted in (**a**) and (**b**)

which make major contribution to the *TCI* value are mainly originated from the ISI distribution, while the long-range ones (>600 ms) are closely linked to the ISI ordering. Since spikes within a burst are correlated with each other in short time scales (Lisman 1997), it might be reasonable to make an inference that burst activities

(defined as a set of spikes with ISI <6 ms in our study, see Koch (Koch et al. 2006)) serve as part of origins of the temporal correlation which contribute to the *TCI* value.

3.3 Relation between spatial- and temporal-correlation

It is clearly listed in Table 1 that in each individual retina, a neuron with large *TCI* value generally has a large *SCI* value. The relationships between *SCI*, *TCI* and burst fraction (percentage of burst activities in a spike train) are plotted in Fig. 5 for the example retina #1. It is clearly shown that in this example retina, spatial correlation shares the same trend with the temporal one, and a neuron firing with higher burst fraction normally has larger *SCI* and *TCI* values (this is also true for other retinas, see also Table 1). Our analysis also suggested that burst activities of a neuron contribute to the *TCI* value. Thus, burst activities may be one of the factors involved in modulation of spatio-temporally correlated network status in the frog retina.

3.3.1 Model prediction and correlation

The above given results suggest that the frog retinal ganglion cells' activities were spatially and temporally correlated. To test whether these spatial and temporal correlations play any role in retinal information processing, we adopted two models—the Coupled Model and the Linear-Nonlinear Model—proposed by Pillow et al. (Pillow et al. 2008) to predict the occurrence of the neuronal spikes, and tested their spike prediction performance. In our analysis, 8 neurons from the example retina were selected for model analysis. The four components (stimulus filter, nonlinear filter, post-spike filter and coupling filter) of the Coupled Model constructed for RGCs from one example retina are illustrated in Fig. 6, whilst only a stimulus filter and a nonlinear filter are included in the Linear-Nonlinear Model.

We applied 200 s experiment data to train the model, and the following 70 s data to test the model prediction. The goodness of prediction of the two different models (quantified by *G* value, see Methods and Materials) are compared in Fig. 7(a), which show that the performance for the Coupled Model is better than that of the Linear-Nonlinear Model. Since both spatial and temporal correlations are related to the burst fraction, we further tested whether burst fraction has relationship with the prediction performance of Models. As shown in Fig. 7(b) and (c), for the Coupled Model, the predictability of the spikes is positively associated with its burst fraction, while this is not the case for the Linear-Nonlinear Model—which implies that burst spikes can be more precisely predicted when considering spatial and temporal correlations.
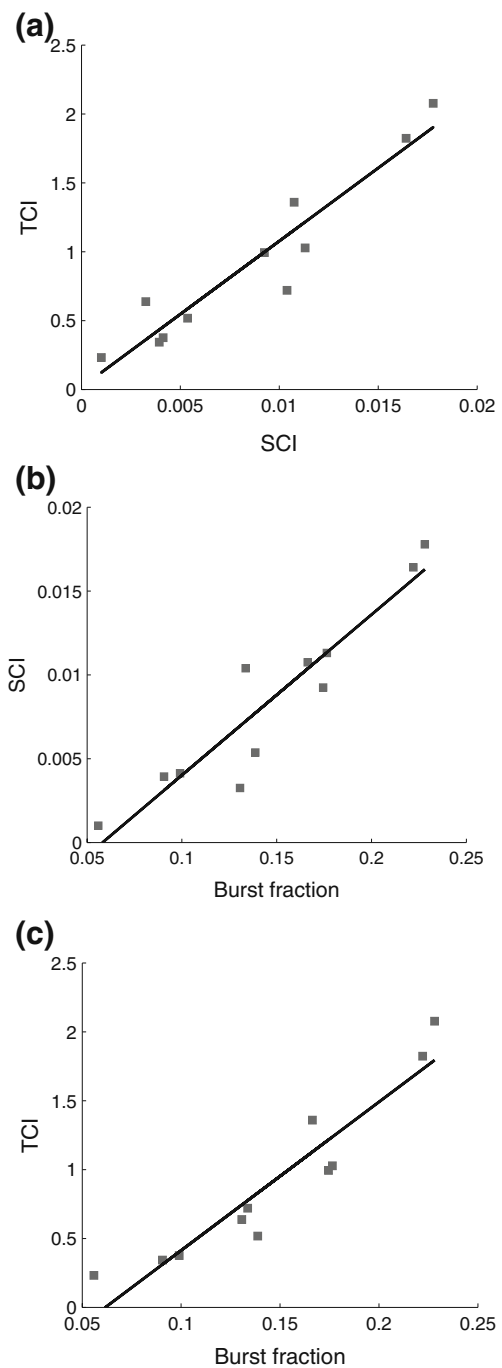

Fig. 5 The relationship between *SCI*, *TCI* values and burst fractions for the 11 neurons selected from the example retina (#1). (a) Relationship between *SCI* and *TCI*; (b) Relationship between burst fraction and *SCI*; (c) Relationship between burst fraction and *TCI*

4 Discussion

The results obtained from the present study were such that spatial and temporal correlations of individual frog RGC were positively correlated with each other and mutually modulated, and that burst activities were involved in the
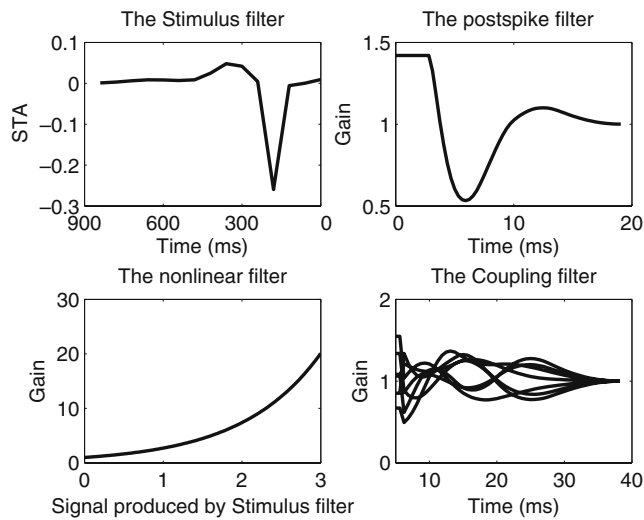
Fig. 6 Four parts of the Coupled Model constructed for one example neuron. The stimulus filter serves for filtering and integrating light from stimulus, the nonlinear filter transforms the signal of stimulus filter to spikes, the post-spike filter captures dependency on the spike-train history, the coupling filter represents the interactions among neighboring spike sequences

modulation of strengths of both spatial and temporal correlations. Given that the pseudo-random checker-board flickering was basically uncorrelated, either spatially or temporally (Cai et al. 2008), it can be inferred that mutual modulation between spatial and temporal correlations in RGCs' activities is mainly owing to the functional organization of the neuronal circuitry. This notion was further tested by using models either cooperating spatial and temporal correlations or not. The results revealed that spikes were predicted more accurately when spatial and temporal correlations were considered, which implies that spatial and temporal correlations originated from intrinsic retinal circuits both contribute to retinal visual information processing.

4.1 Spatial correlation

Spatial correlation between neuronal activities has been extensively studied (DeVries 1999; Liu et al. 2007; Shlens et al. 2008), and it has been well accepted that concerted firings among neurons play an important role in retinal information processing. It was reported previously that concerted firings were able to encode more detailed visual information (Meister et al. 1995; Schnitzer and Meister 2003); what's more, correlated activities of retinal neurons may drive their common post-synaptic neurons in lateral geniculate nucleus (LGN) more effectively and more efficiently (Field and Chichilnisky 2007; Usrey et al. 1998).

Our present result shows that in the frog retina, RGCs' status can be characterized by *SCI*—neurons with bigger
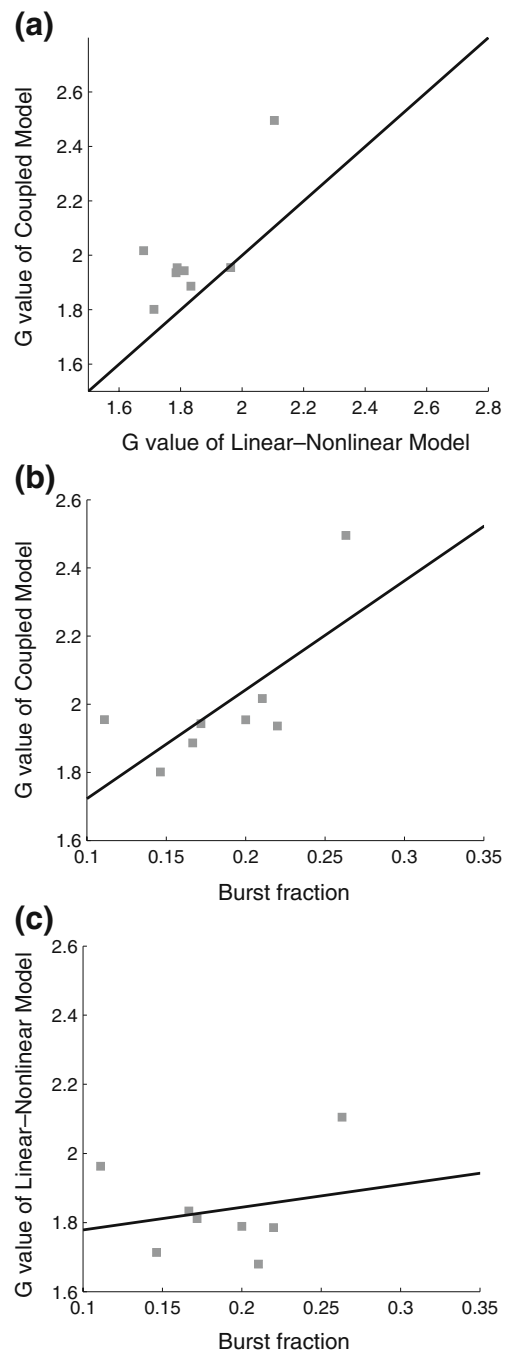

Fig. 7 (a) Goodness of prediction of the Coupled Model and the Linear-Nonlinear Model; (b) Relationship between the burst fraction of the spike trains and the spike prediction performance of the Coupled Model; (c) Relationship between the burst fraction of the spike trains and the spike prediction performance of the Linear-Nonlinear Model

SCI values share stronger spatial correlations with their neighboring neurons, while those with smaller *SCI* values are weakly correlated with other neurons. It was also observed that a neuron with bigger *SCI* generally fires

more burst activities, which suggests that these two aspects of neuronal activities are correlated to each other. On the one hand, burst activities of an RGC can be partially resulted from intensive pre-synaptic inputs (Lisman 1997), parallel signals of which are also sent to its neighboring ganglion cells due to the network wirings. Such "indirect" connections among ganglion cells via the pre-synaptic interneurons may result in a strong correlation status of the cells. On the other hand, neighboring neurons can excite each other via gap junctions to produce synchronous firing. Given the fact that gap junctional conductance is dependent on the voltage-difference between the cells (Bloomfield and Völgyi 2009), bursting activities of one neuron are more likely to excite its neighboring neurons via the gap junction, as compared to isolated spikes (Snider et al. 1998), which in turn results in increased correlation strength between the neurons and enhance the spatial correlation strength.

4.2 Temporal correlation

Temporal correlation was thought to play an important role in information transmission in neural systems (Buonomano and Maass 2009). It was proposed that in guinea pig retinal ganglion cells, temporal correlation within a spike train could improve coding performance in the presence of noise (Koch et al. 2004). What's more, it was reported that the retinal ganglion cells were able to encode visual information in a predictive way (Hosoya et al. 2005), which implies that at RGC layer, information coding is not only based on the present stimulus input but also the recent status of the neurons. In this sense, temporal correlation could serve as "memory" for forgoing stimulus, making the "predictive" way of coding behavior possible.

In the present study, it was found that temporal correlation also exists in the frog retinal ganglion cells. The analytical results showed that temporal correlation in short-range (less than 600 ms) and long-range (longer than 600 ms) co-existed within single spike trains. ISI distribution and ISI ordering are both factors affecting temporal correlation of a spike train, with the short-range correlation more linked to ISI distribution, while the long-range ones more dependent on the ISI ordering. However, the TCI value of a spike train was more attributed to its short-range temporal correlation—thus more linked to its ISI distribution, among which the effect of burst fraction can play a part.

Since it is well accepted that spikes within a burst are temporally correlated (Koch et al. 2006; Lisman 1997), thus big burst fraction of a neuron reasonably leads to big TCI value. On the other hand, the TCI value is less dependent on the ISI ordering which contributes to long-range temporal correlation. One possible explanation might be

that the physiological function of the retina is to rapidly process visual information and send it to the central visual part for further processing; which requires the so-called "predictive" coding in the retina occur at a short time scale. And this is in consistent with our observation that TCI value of a spike train is more correlated with short-range correlation than the long-range one, while the long-range correlation might be more related to the intrinsic characteristics of neural systems (Bhattacharya et al. 2005).

4.3 Relationship between SCI and TCI and model prediction

In the present study, it was observed that the SCI and TCI values were positively correlated: a neuron with big SCI value was more likely to have a big TCI value, and vice versa. Besides, model based examination revealed that the Coupled Model considering spatial and temporal correlations could predict spikes more accurately than the Linear-Nonlinear Model without any correlation considered. These results further support the notion that spatial and temporal correlation among the retinal ganglion cells contribute to information coding. In addition, the SCI and TCI values for a neuron were both highly correlated with its burst fraction, and a spike sequence could be better predicted by the Coupled Model when it had more burst spikes, which further confirms the role of burst activities in connecting spatial and temporal correlations. Spikes in burst were reported more reliable as to propagation of information (Lisman 1997) than others; the finding of the correlation between burst activities and spatial and temporal correlation indices of a neuron may add new insight to the function of burst.

As to the functional role of spatial and temporal correlations, it was reported that the spatial and temporal correlations could improve retina's coding capacity (Pillow et al. 2008). Intuitively, spatially correlated activities contribute to encode continuous or coherent spatial features of visual stimulus (Neuenschwander and Singer 1996), whilst temporally correlated activities contribute to encode the temporally changing features of visual stimulus (Lesica and Stanley 2004). Our results further show that these two kinds of correlations are not independent of each other, they are mutually modulated. Such spatio-temporally correlated activities might be vital for retinal neurons to process visual information efficiently, particularly in natural visual environment which is constructed by spatio-temporally correlated visual images.

References

Bhattacharya, J., Edwards, J., Mamelak, A. N., & Schuman, E. M. (2005). Long-range temporal correlations in the spontaneous spiking of neurons in the hippocampal-amygdala complex of humans. *Neuroscience, 131*(2), 547–555.

Bloomfield, S. A., & Völgyi, B. (2009). The diverse functional roles and regulation of neuronal gap junctions in the retina. *Nature Reviews. Neuroscience, 10*(7), 495–506.

Brivanlou, I. H., Warland, D. K., & Meister, M. (1998). Mechanisms of concerted firing among retinal ganglion cells. *Neuron, 20*(3), 527–540.

Buonomano, D. V., & Maass, W. (2009). State-dependent computations: spatiotemporal processing in cortical networks. *Nature Reviews. Neuroscience, 10*(2), 113–125.

Cai, C. F., Zhang, Y. Y., Liu, X., Liang, P. J., & Zhang, P. M. (2008). Detecting determinism in firing activities of retinal ganglion cells during response to complex stimuli. *Chinese Physics Letters, 25*(5), 1595–1598.

DeVries, S. H. (1999). Correlated firing in rabbit retinal ganglion cells. *Journal of Neurophysiology, 81*(2), 908–920.

Devries, S. H., & Baylor, D. A. (1997). Mosaic arrangement of ganglion cell receptive fields in rabbit retina. *Journal of Neurophysiology, 78*(4), 2048–2060.

Field, G. D., & Chichilnisky, E. J. (2007). Information processing in the primate retina: circuitry and coding. *Annual Review of Neuroscience, 30*, 1–30.

Hosoya, T., Baccus, S. A., & Meister, M. (2005). Dynamic predictive coding by the retina. *Nature, 436*(7047), 71–77.

Ishikane, H., Gangi, M., Honda, S., & Tachibana, M. (2005). Synchronized retinal oscillations encode essential information for escape behavior in frogs. *Nature Neuroscience, 8*(8), 1087–1095.

Jing, W., Liu, W. Z., Gong, X. W., Gong, H. Q., & Liang, P. J. (2010a). Influence of GABAergic inhibition on concerted activity between the ganglion cells. *NeuroReport, 21*(12), 797–801.

Jing, W., Liu, W. Z., Gong, X. W., Gong, H. Q., & Liang, P. J. (2010b). Visual pattern recognition based on spatio-temporal patterns of retinal ganglion cells' activities. *Cognitive Neurodynamics, 4*, 179–188.

Koch, K., McLean, J., Berry, M., Sterling, P., Balasubramanian, V., & Freed, M. A. (2004). Efficiency of information transmission by retinal ganglion cells. *Current Biology, 14*(17), 1523–1530.

Koch, K., McLean, J., Segev, R., Freed, M. A., Berry, M. J., Balasubramanian, V., et al. (2006). How much the eye tells the brain. *Current Biology, 16*(14), 1428–1434.

Lesica, N., & Stanley, G. (2004). Encoding of natural scene movies by tonic and burst spikes in the lateral geniculate nucleus. *The Journal of Neuroscience, 24*(47), 10731.

Lettvin, J., Maturana, H., McCulloch, W., & Pitts, W. (1959). What the frog's eye tells the frog's brain. *Proceedings of the IRE, 47*(11), 1940–1951.

Lisman, J. E. (1997). Bursts as a unit of neural information: making unreliable synapses reliable. *Trends in Neurosciences, 20*(1), 38–43.

Liu, X., Zhou, Y., Gong, H. Q., & Liang, P. J. (2007). Contribution of the GABAergic pathway (s) to the correlated activities of chicken retinal ganglion cells. *Brain Research, 1177*, 37–46.

Lowen, S. B., & Teich, M. C. (1992). Auditory-nerve action potentials form a nonrenewal point process over short as well as long time scales. *Journal of the Acoustical Society of America, 92*(2I), 803–806.

Meister, M., Pine, J., & Baylor, D. A. (1994). Multi-neuronal signals from the retina: acquisition and analysis. *Journal of Neuroscience Methods, 51*(1), 95–106.

Meister, M., Lagnado, L., & Baylor, D. A. (1995). Concerted signaling by retinal ganglion cells. *Science, 270*(5239), 1207.

Neuenschwander, S., & Singer, W. (1996). Long-range synchronization of oscillatory light responses in the cat retina and lateral geniculate nucleus. *Nature, 379*(6567), 728–733.

Oram, M., Wiener, M., Lestienne, R., & Richmond, B. (1999). Stochastic nature of precisely timed spike patterns in visual system neuronal responses. *Journal of Neurophysiology, 81*(6), 3021–3033.

Pillow, J. W., Shlens, J., Paninski, L., Sher, A., Litke, A. M., Chichilnisky, E. J., et al. (2008). Spatio-temporal correlations and visual signalling in a complete neuronal population. *Nature, 454*(7207), 995–999.

Reid, R., Victor, J., & Shapley, R. (1997). The use of m-sequences in the analysis of visual neurons: linear receptive field properties. *Visual Neuroscience, 14*(06), 1015–1027.

Reinagel, P., & Reid, R. C. (2000). Temporal coding of visual information in the thalamus. *The Journal of Neuroscience, 20*(14), 5392.

Schneidman, E., Berry, M. J., II, Segev, R., & Bialek, W. (2006). Weak pairwise correlations imply strongly correlated network states in a neural population. *Nature, 440*(7087), 1007.

Schnitzer, M. J., & Meister, M. (2003). Multineuronal firing patterns in the signal from eye to brain. *Neuron, 37*(3), 499–511.

Segev, R., Goodhouse, J., Puchalla, J., & Berry Ii, M. J. (2004). Recording spikes from a large fraction of the ganglion cells in a retinal patch. *Nature Neuroscience, 7*(10), 1154–1161.

Shlens, J., Rieke, F., & Chichilnisky, E. J. (2008). Synchronized firing in the retina. *Current Opinion in Neurobiology, 18*(4), 396–402.

Snider, R., Kabara, J., Roig, B., & Bonds, A. (1998). Burst firing and modulation of functional connectivity in cat striate cortex. *Journal of Neurophysiology, 80*(2), 730–744.

Strong, S., Koberle, R., van Steveninck, R., & Bialek, W. (1998). Entropy and information in neural spike trains. *Am Phys Soc, 80*, 197–200.

Teich, M. C., Turcott, R. G., & Siegel, R. M. (1996). Temporal correlation in cat striate-cortex neural spike trains. *IEEE Engineering in Medicine and Biology Magazine, 15*(5), 79–87.

Teich, M. C., Heneghan, C., Lowen, S. B., Ozaki, T., & Kaplan, E. (1997). Fractal character of the neural spike train in the visual system of the cat. *Journal of the Optical Society of America A, 14*(3), 529–546.

Usrey, W. M., Reppas, J. B., & Reid, R. C. (1998). Paired-spike interactions and synaptic efficacy of retinal inputs to the thalamus. *Nature, 395*(6700), 384–387.

Zhang, P. M., Wu, J. Y., Zhou, Y., Liang, P. J., & Yuan, J. (2004). Spike sorting based on automatic template reconstruction with a partial solution to the overlapping problem. *Journal of Neuroscience Methods, 135*(1–2), 55–65.